31st Annual International Conference of the IEEE EMBS
Minneapolis, Minnesota, USA, September 2-6, 2009

Modeling the Temperature Dependence of Thermophysical Properties: Study on the Effect of Temperature Dependence for RFA

Hiroki Watanabe, Yo Kobayashi, Makoto Hashizume, and Masakatsu G. Fujie, *Members, IEEE*

***Abstract* — Radio frequency ablation (RFA) has increasingly been used over the past few years and RFA treatment is minimally invasive for patients. However, it is difficult for operators to control the precise formation of coagulation zones due to inadequate imaging modalities. With this in mind, an ablation system using numerical simulation to analyze the temperature distribution of the organ is needed to overcome this deficiency. The objective of our work is to develop a temperature dependent thermophysical liver model.**

First, an overview is given of the development of the thermophysical liver model. Second, a simulation to evaluate the effect of temperature dependence of the thermophysical properties of the liver is explained. Finally, the result of the simulation, which indicated that the temperature dependence of thermophysical properties accounts for temperature differences influencing the accuracy of RFA treatment is described.

I. Introduction

A. Radio frequency ablation (RFA) for liver cancer

Radio frequency ablation is an important method for treating liver tumors, which has increasingly been used over the past few years. RFA involves an electrode being percutaneously introduced into the tumor and RF energy being applied, whereupon the temperature of the tissue rises due to the ionic agitation generated by the microwaves. Tissue coagulation occurs as a result of protein denaturation when the tissue around the electrode reaches a temperature of around $60\,°C$. Subsequently, moisture evaporation occurs and the tumors become completely necrotic at 70-80 $°C$. This percutaneous procedure, which has proved its effectiveness and safety, also has the advantage of being minimally invasive, meaning lower impact operations and shorter hospital stays.

Manuscript received April 7, 2009. This work was supported in part by the following organizations: "Establishment of the Consolidated Research Institute for Advanced Science and Medical Care," Encouraging Development Strategic Research Centers Program, Special Coordination Funds for Promoting Science and Technology, Ministry of Education, Culture, Sports, Science and Technology, Japan; the Global Century Center of Excellence (COE) Program "Global Robot academia," Waseda University, Tokyo, Grant-in-Aid for 2009, 21700513;

H. Watanabe is with the Graduate School of Science and Engineering, Waseda University, Japan. (59-309, 3-4-1, Okubo, Shinjuku Ward, Tokyo, Japan, tel: +81-3-5286-3412; fax: +81-3-5291-8269; e-mail: hiroki_watanabe@suou.waseda.jp)

Y. Kobayashi, a member of the Faculty of Science and Engineering, is with the Graduate School of Science and Engineering, Waseda University, Japan.

M. Hashizume is with the Center for the Integration of Advanced Medicine and Innovative Technology, Kyushu University Hospital, Japan.

M.G. Fujie, a member of the Faculty of Science and Engineering, is with the Graduate School of Science and Engineering, Waseda University, Japan.

B. Practical shortcomings of RFA

Although RFA is minimally invasive treatment, it does has some shortcomings such as 1) inadequate imaging modalities, 2) non-optimized power supply to form an adequate ablation area, and 3) the inability to form an ablation area of sufficient size for large tumors.

These shortcomings make it difficult to control the precise formation of coagulation zones, meaning the area is only sufficient to cover the tumor and surrounding safety area. In addition, complications such as burns to neighboring organs or the bile duct often occur due to excessive heat transfer. These problems are crucial for the patients because tumors often recur from areas that have not been fully cauterized [1].

C. Robot-assisted RFA Therapy

In recent years, considerable research has been carried out on surgical robots and navigation systems for minimally invasive and precise surgery [2]-[3]. The majority has been focused solely on robot systems based on kinematics, dynamics and material mechanics to facilitate the precise control of manipulators. However, in clinical practice, as well as robot modeling approaches, organ modeling approaches such as thermo dynamic or fluid dynamic, are also now required. The use of a surgical robot may enable the position of the needle to be controlled and enhance the accuracy of its insertion into the tumor. However, these systems are unable to supply sufficient electrical power to the needle to form an ablation area of the required size.

The purpose of our study is thus to develop a robotic system to assist RFA therapy (Fig. 1), which includes some thermo dynamic functions to solve the shortcomings of conventional RFA treatment summarized in Section I-B.

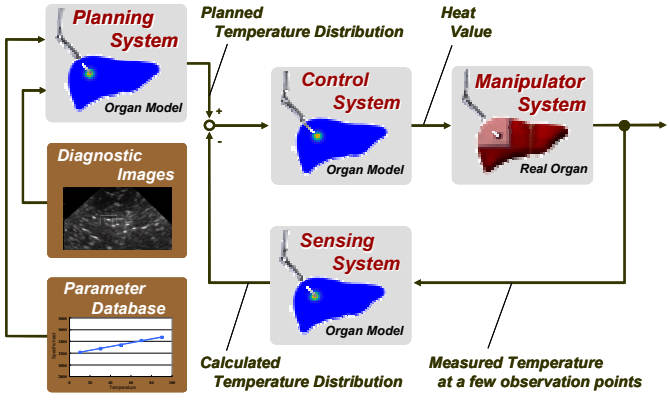

Fig. 1 Robot assisted RFA therapy

This robotic system is composed of the following three key systems based on the organ model, while the system concept is proposed by Kobayashi et al. [4]-[7]:

1) Model based planning system: The model based planning system realizes the provision of precise information, including the ideal state of temperature distribution around the tumor during the operation. Accordingly, the use of the system makes it possible to plan the treatment procedure preoperatively.

2) Model based control system: The model based control system realizes the control and supply of an adequate amount of electrical power to the RFA electrode. This system enables a coagulation zone of optimal size to form around the tumor.

3) Model based sensing system: The model based sensing system realizes the calculation of temperatures in all areas of the organ based on information concerning the temperature measured at a few observation points using a thermo sensor. This system enables the operator to determine the real time temperature in the affected area as information to assist in navigating the operation.

D. Thermophysical model of the organ

The thermophysical model is constructed from two essential components, one of which is a reliable database of the thermophysical properties of the organ, such as specific heat and thermal conductivity. The other is an accurate temperature distribution simulator based on FEM. It is important for the accurate simulator to use the proper thermophysical properties of the organ. However, creating an accurate thermophysical model was a challenging problem because of the complexities of the thermophysical properties of the organ. One of the most complicated phenomena in the organ is the fact that the thermophysical properties, such as the specific heat and the thermal conductivity, change according to the tissue temperature. The specific heat and thermal conductivity are included in the bio heat equation (1); required to calculate the tissue temperature around the tumor [8]-[18].

$$\rho c \frac{\partial \theta}{\partial t} = \lambda \nabla^2 \theta + \sigma \left| E \right|^2 - \rho \rho_b c_b F (\theta - \theta_b) + Q_m \qquad (1)$$

where ρ is the density of the organ [kg/m^3], c is its heat capacity [J/kgK], θ its temperature [$^\circ C$], λ its thermal conductivity [W/mK], σ its electrical conductivity [S/m], E its electrical field [V/m], ρ_b the density of blood, c_b the heat capacity of blood, F the blood perfusion coefficient of the organ [m^3/kgs], θ_b the blood temperature, and Q_m the metabolic heat source term of the organ [W/m^3].

Webster et al. and Wolf et al. have also indicated that the temperature dependence of the thermophysical properties of the organ has some effect on the accuracy of the temperature distribution simulator for RFA [19] [20]. However, this research has not revealed any effect on the simulation result based on the temperature dependence of these properties on a quantitative basis.

The originality of our work is the development of a temperature dependent liver model based on the detailed thermophysical properties of tissue. For some thermophysical properties of the organ, we already measured the temperature dependence of the thermal conductivity of hog liver and reported the same in the previous paper [1]. In this paper, the newly-measured and modeled temperature dependence of specific heat of hog liver is shown, as well as the temperature dependence of thermal conductivity. In addition, this paper focuses on the effect on the simulation result of the temperature dependence of thermophysical properties.

This report is organized as follows: Section II presents the measurements and modeling of the temperature dependence of the specific heat and thermal conductivity of hog liver. Section III explains the simulation of the temperature distribution during RFA and evaluation of the inevitable effect of the temperature dependent properties. Finally, Section IV presents our conclusions and plans for future work.

II. Thermophysical Model of the Liver

The temperature dependence of the specific heat and thermal conductivity of hog liver were measured and modeled from the experiments.

A. Specific heat of the liver

1) Method: Generally speaking, the linear heating method based on Differential Scanning Calorimetry technology (DSC) is carried out to measure the specific heat of high-molecular, organic or inorganic materials. In this method, the sample is linearly heated up with the device, and the specific heat of the former is calculated based on its temperature change. However, when this method is used, it is very difficult to measure the accurate specific heat of materials consisting of protein and becoming denatured at a specific temperature range. This is because the total amount of heat flow provided to the sample by the device is used not only to change the tissue temperature of the sample but also for the endothermic reaction due to the protein denaturation. Therefore, a method that cancels the amount of the endothermic heat flow due to the protein denaturation is required to measure the accurate specific heat of materials comprising protein components.

With this in mind, in order to measure the accurate specific heat of the hog liver, we performed the Sine-wave heating method based on the Modulated Differential Scanning Calorimetry technology (MDSC) using DSC (TA Instrument Q2000) that eliminates the influence of the endothermic reaction from the calculation process on specific heat, as well as the linear heating method.

2) Results and modeling: The result of the specific heat of the hog liver using both the linear heating method and the Sine-wave heating method is shown in Fig. 2.

Figure 2 shows that the result for specific heat increased rapidly from about 50 $^\circ C$ when the linear heating method was used. On the other hand, due to the Sine-wave heating method, the specific heat increased linearly throughout the entire temperature range.

It is generally known that when measuring the specific heat of protein-based materials using the linear heating method, the specific heat of the materials begins to increase rapidly when

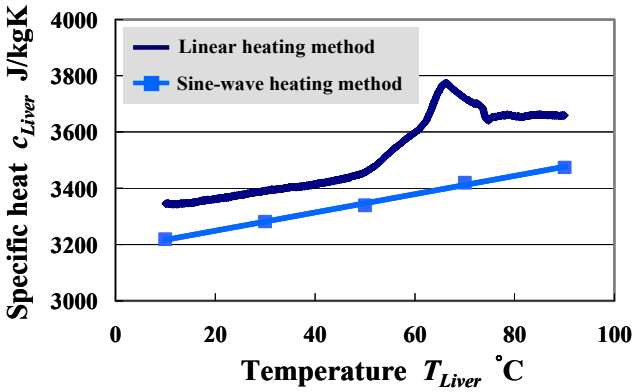

Fig. 2 Temperature dependence of specific heat

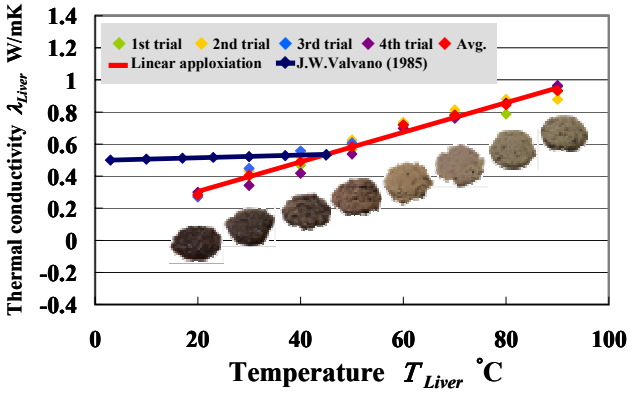

Fig. 3 Temperature dependence of thermal conductivity

the protein becomes denatured. This is because the specific heat is calculated in this method as if all of the heat provided by the device were used only to change the material temperature; despite the fact part of it is used to handle the endothermic reaction due to the protein denaturation. So the correct value of specific heat measured by the Sine-wave heating method is generally lower than that measured by the linear heating method. In the same way in Fig. 3, it was confirmed that the Sine-wave heating method could cancel out the effect of protein denaturation, and be used to derive the correct value of the specific heat of hog liver. The relation between temperature T_{Liver} and specific heat c_{Liver} is modeled as equation (2):

$$c_{Liver} = a_1 T_{Liver} + b_1 \tag{2}$$

Where a_1 is 3.2 [J/kgK^2] and b_1 is 3.2 x 10^3 [J/kgK].

B. Thermal conductivity of the liver

1) Method: Generally speaking, two main methods are used to obtain the thermal conductivity of any materials. One category includes unsteady methods, such as the hot wire and laser flush methods, while examples of so-called "steady" methods include the comparative method and heat flow meter method. Among these, the latter has been widely used for biological tissue. This method involves measuring the thermal conductivity by sensing the temporal temperature change of a heated thermistor inserted into a sample [21].

Valvano et al. have obtained the temperature dependence of the thermal conductivity of hog liver using the hot wire method [22]. In their research, the thermal conductivity of hog liver was measured from 3 to 45 $^{\circ}C$. Valvano's experimental results show that the thermal conductivity increases when the temperature rises, and linear approximation was used to fit the measurements. The experiment was carried out only below 45 $^{\circ}C$, but the temperature of the affected area reaches up to about 90 $^{\circ}C$ relative to body temperature during RFA treatment, Therefore, data at least from 36 (body temperature) to 90 $^{\circ}C$ is necessary for an accurate thermophysical model of the liver. For this reason, we measured the thermal conductivity of a hog liver from 20 to 90 $^{\circ}C$ using the steady comparative method, which is suitable for measuring thermal conductivity within a high temperature range.

2) Results and modeling: Figure 3 shows the thermal conductivity of the hog liver obtained from four trials, the average value of the latter, and the experimental results obtained by Valvano. According to the result of our work in Fig. 3, the thermal conductivity of hog liver linearly increased within the range 20 to 90 $^{\circ}C$. This result probably stems from the reduced moisture as the temperature rises. The appearance of the sample at each temperature is also shown in Fig. 3. As these pictures show, tissue degeneration increases as the temperature increases**.** Specifically, liver tissue retains considerable moisture from 20 to 40 $^{\circ}C$, but the water content diminishes at above 50 $^{\circ}C$. This may be due to the protein denaturation and coagulation of the tissue. Via our experiment, the relation between temperature T_{Liver} and thermal conductivity λ_{Liver} was modeled as an equation (3):

$$\lambda_{Liver} = a_2 T_{Liver} + b_2 \tag{3}$$

Where a_2 is 9.2 x 10^{-3} [W/mK^2] and b_2 is 1.2 x 10^{-1}[W/mK].

3) Discussions: Figure 3 shows the difference in measured values between Valvano's study and this one within the range 20 to 45 $^{\circ}C$. This difference is considered to stem from individual differences in samples and the difference of experimental principle between the hot wire and comparative methods. Detailed research on the effect of these differences should be carried out to construct a highly accurate thermophysical model of the organ.

III. VALIDATION

To investigate the effect of the temperature dependence of thermophysical properties of the liver on the temperature distribution during RFA, we evaluated how the differences occur in the simulation of the two liver models: (A) A temperature independent liver model, which has constant specific heat and thermal conductivity based on the previous work, (B) A temperature dependent liver model, which has non-constant specific heat and thermal conductivity obtained from experiments described in Section II. In this study, two-dimensional FEM analysis was developed. This simulator calculates the two-dimensional temperature distribution around the electrode when a certain amount of heat, which is supposed to be joule heat due to radiofrequency waves, is allowed to flow into the model.

A. Temperature distribution simulator based on FEM

We evaluated the extent of the temperature differences appearing around the electrode between the two liver models with this simulator. In the following sentence, the fundamental formulation and solution of the simulator is described.

As the first step for constructing the finite element equation, Pennes' bio heat equation (1) is spatially discretized as equation (4) using the Galerkin method:

$$[C]\frac{\partial\{T\}}{\partial t}+[K]\{T\}=\{F\} \tag{4}$$

Where $\{T\}$ is the temperature vector at each element, $[C]$ is the heat capacity matrix, including the specific heat of the liver, $[K]$ is the heat conductivity matrix, including the thermal conductivity of the liver and $\{F\}$ is a heat flux vector including the heat flow supplied by the electrode and that absorbed by blood.

Secondly, equation (4) is temporarily discretized as equation (5) with the Crank-Nikolson method:

$$\left(\frac{1}{\Delta t}[C]+\frac{1}{2}[K]\right)\{T_n\} = \left(\frac{1}{\Delta t}[C]-\frac{1}{2}[K]\right)\{T_{n-1}\}+\{F\} \tag{5}$$

Where n is the number of calculations and Δt the time span for a calculation.

Using the LU decomposition, equation (5) is sequentially solved for $\{T_n\}$. In this case, the temperature dependence of specific heat and the thermal conductivity of the liver were reflected in the simulation by updating $[C]$ and $[K]$ based on the previously calculated temperature $\{T_{n-1}\}$ and equation (2), (3).

B. Simulation conditions

The analytical models were a temperature independent hog liver model (A) and a temperature dependent hog liver model (B). Both (A) and (B) were 100 [mm] squared in lengths and supposed to be heated at 2.5×10^6 [W/m^3] with the electrode from the 20 nodes located at the center of the models. The initial thermal condition in all elements and the thermal boundary condition at the surface of the model are also T=37 °C .

Table 1 Parameters of simulation

Density ρ_{Liver} [kg/m^3]	1060
Specific heat c_{Liver} [J/kgK] (A)	3600
Specific heat c_{Liver} [J/kgK] (B)	$a_1T_{Liver}+b_1$
Thermal conductivity λ_{Liver} [W/mK] (A)	0.502
Thermal conductivity λ_{Liver} [W/mK] (B)	$a_2T_{Liver}+b_2$
Density ρ_{Blood} [kg/m^3]	1000
Specific heat c_{Blood} [J/kgK]	4180
Blood coefficient ω [1/s]	6.4 x 10^{-3}
Heat flow from the electrode $Q_{electrode}$ [W/m^3]	2.5 x 10^6
Initial temperature at all elements °C	37
Boundary temperature °C	37

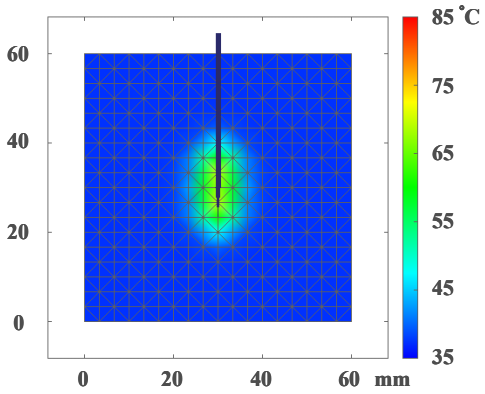

(a) Temperature independent liver model (Time=60 [s])

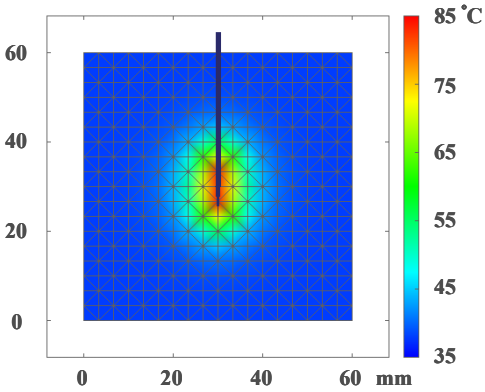

(b) Temperature independent liver model (Time=600 [s])

Fig. 4 Simulation results of the temperature-independent liver model (A)

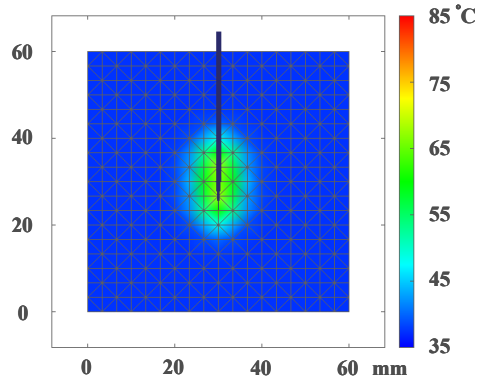

(a) Temperature dependent liver model (Time=60 [s])

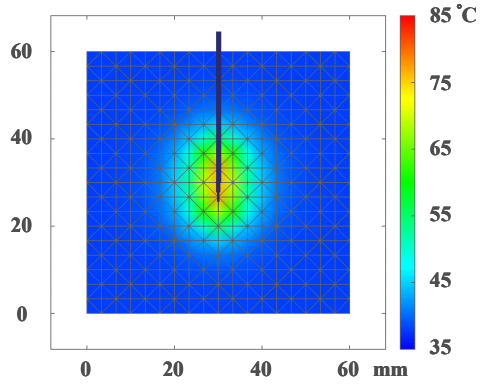

(b) Temperature dependent liver model (Time=600 [s])

Fig. 5 Simulation results of temperature-dependent liver model (B)

C. Thermophysical properties of the liver model

The thermophysical properties and simulation conditions used in this simulation are shown in Table 1. In the simulation, the specific heat c_{Liver} and thermal conductivity λ_{Liver} of the temperature independent liver model (A) were set to c_{Liver}=3600 [J/kgK] and λ_{Liver}=0.502 [W/mK] from Duck [23] respectively, as quoted by Chang [8]. These values were set to be constant during the simulation. Moreover, for the temperature dependent model (B), these properties were set to $c_{Liver}=a_1T_{Liver}+b_1$ [J/kgK] and $\lambda_{Liver}=a_2T_{Liver}+b_2$ [W/mK], based on equations (2) and (3). In addition, there is assumed to be capillary blood into the liver in both models. Subsequently, the blood perfusion effects were set and taken into account based on the blood data by Tungjitkusolmum et al. [24].

D. Simulation results

Figures 4 and 5 show examples of the simulation results at 60 [s] and 600 [s] respectively. The results in Figs. 4 and 5 show no significant difference in temperature between the two liver models around the electrode at 60 [s], while it is confirmed that the temperature around the electrode of the temperature independent model (A) becomes higher than that of the temperature dependent model (B) at 600 [s].

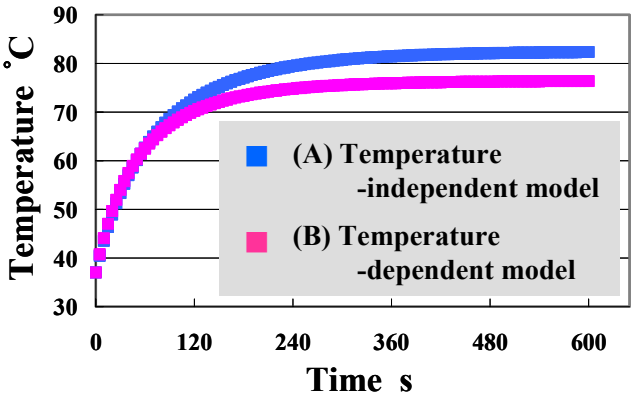

Fig. 6 Temporal temperature at the center of the heat source

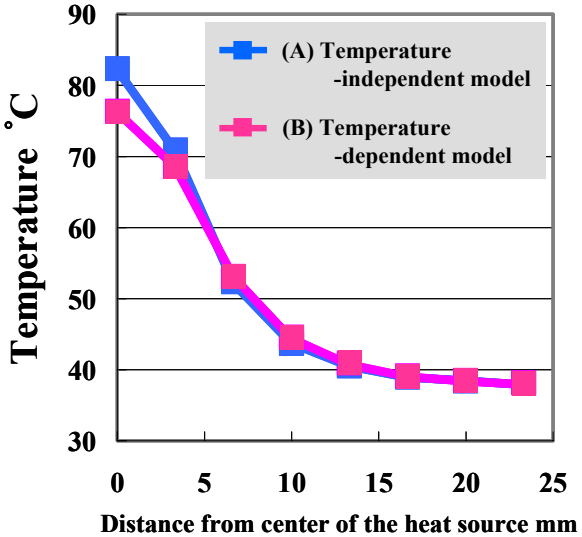

Fig. 7 Spatial temperature change at the steady state (600s)

In this regard, Fig. 6 shows a temporal temperature change at the center of the heat source by the electrode. Fig. 6 shows that the temperature at the center of the heat source increases rapidly from 37 to 60 $°C$ in both models, while both increase rates decreased above 60 $°C$. In addition there is no temperature difference between the two models below about 60 $°C$, while the temperature difference increases rapidly above about 60 $°C$. The difference results in about 6 $°C$ at the steady state.

Next, Fig. 7 describes the spatial temperature change at each distance from the center of the heat source at the steady state (600 s). Fig. 7 shows little temperature difference below 60 $°C$ between the two models. Moreover, this tendency is confirmed at an area farther than 5 mm from the center of the electrode, while there were temperature differences between the two liver models nearer than 5 mm from the center of the electrode, the temperature of which exceeds 60 $°C$.

Consequently, the simulation results are summarized as follows:

1) Near the electrode where the temperature exceeds 60 $°C$: There are differences ranging from 0 to 6 $°C$ in the simulation results between the temperature dependent hog liver model and the temperature independent hog liver model

2) Far from the electrode, the temperature of which is below 60 $°C$: There are no notable temperature differences in the simulation results between the temperature dependent and independent hog liver models respectively.

E. Discussion

During RFA treatment, only regions maintained above 70 $°C$ for 8-10 minutes are regarded as fully ablated. If any areas remain that are not sufficiently ablated under this ablation condition, the risk of recurrence soars. Based on the validation results described in Section III-D, the temperature dependence of the thermophysical properties of the liver results in a difference of 0-6 $°C$ above 60 $°C$ when compared with the results of the simulation in which the thermophysical properties of the liver are temperature independent. This means that the risk of issuing the wrong temperature estimation may be derived when we use the temperature distribution simulator with a temperature independent liver model during practical RFA; It is extremely dangerous to consider an area which is not actually fully heated up as one that has been sufficiently heated for coagulation. Therefore, it can be considered vital for the accuracy of RFA treatment to consider the temperature dependence of the thermophysical properties of the liver.

On the other hand, as future work, we should carry out a more detailed validation, such as in vitro experiments using isolated hog livers, in order to evaluate the effect of the temperature dependence of the thermophysical properties of the liver. Moreover, the simulator must also be improved, because many other phenomena regarding the temperature dependence of the thermophysical properties of the liver remain unclear in RFA. For example, when there are large vessels near the tumor, these absorb heat from the electrode and the tumor is not sufficiently heated. In this case, there is a

possibility of the thermal conductivity of the liver decreasing due to the low temperature of the tissue. As a result, heat is hardly conducted into the liver. With this in mind, we should improve the simulator which calculates the temperature around the tumor when there are large vessels near the latter. Moreover, the internal pressure of the tumor is said to increase rapidly and the liver burst as a result of inner high pressure when the tumor is rapidly heated and the temperature drastically rises. In this case, the splattered tissue is the catalyst for the recurrence of cancer. The relation between temperature and internal pressure must therefore be clarified to ensure a more reliable simulator for RFA.

IV. Conclusions and Future Work

This paper presents modeling concerning the temperature dependence of the thermophysical properties of the liver and a simulation conducted to evaluate the effect of the temperature dependent liver model is shown. First, detailed explanations of the experiment performed to measure the thermophysical properties of the liver are shown. As a result, the relation between the temperature and thermophysical properties was linearly approximated. Next, temperature distribution simulations were conducted in order to evaluate how the difference appears on the temperature distribution from the two liver models: (A) Temperature independent liver model, (B) Temperature dependent liver model. The simulation results show that the temperature dependent liver model accounts for temperature differences, which influences the accuracy of RFA when compared with the temperature independent liver model. In future therefore, an improved simulator and a more detailed validation of the effect of temperature dependence of thermophysical properties are necessary. For example, a simulator with large vessels around the tumor should be constructed and the effect of inner pressure should be taken into account. Moreover, in vitro experimental validation with thermocouple and thermography, will be carried out. Finally, a thermophysical liver model, including the accurate thermophysical properties of the liver and an accurate temperature distribution simulator, will be involved in the model based following three systems; 1) model based planning system, 2) model based control system, 3) model based sensing system. Moreover, organ model based ablation systems will be further developed for use in safe and precise clinical treatment.

References

[1] H. Watanabe, Y. Kobayashi, M. G. Fujie, "Modeling the Temperature Dependence of Thermal Conductivity: Developing a System for Robot-Assisted RFA therapy", in Proceedings of the 2nd IEEE/RAS-EMBS International Conference on Biomedical Robotics and Biomechatronics, pp. 483-488, 2008.

[2] R. H. Taylor and D. Stoianovici "Medical Robotics in Computer-Integrated Surgery", IEEE Transactions on Robotics and Automation,Vol. 19, No. 5, pp. 765-781,2003.

[3] P. Daraio, B. Hannaford and A. Menciassi, "Smart Surgical Tools and Augmenting Devices", IEEE Transactions on Robotics and Automation, Vol. 19, No. 5, pp. 782-792,2003.

[4] Y. Kobayashi, J. Okamoto, M. G. Fujie, "Physical Properties of the Liver for Needle Insertion Control" , In IEEE International Conference on Intelligent Robotics and Systems (2004) , pp. 2960-2966, 2004.

[5] Y. Kobayashi, J. Okamoto, M.G. Fujie, "Physical Properties of the Liver and the Development of an Intelligent Manipulator for Needle Insertion", In IEEE International Conference on Robotics and Automation (2005), pp. 1644-1651, 2005.

[6] Y. Kobayashi, A. Onishi, T. Hoshi, K. Kawamura and M. G. Fujie, "Viscoelastic and Nonlinear Organ Model for Control of Needle Insertion Manipulator", in Proceeding of the 29th Annual International Conference of the IEEE Engineering in Medicine and Biology Society, pp. 1242-1248, 2007.

[7] Y. Kobayashi, A. Onishi, T. Hoshi, K. Kawamura and M. G. Fujie, "Deformation Simulation using a Viscoelastic and Nonlinear Organ Model for Control of a Needle Insertion Manipulator", in Proceedings of 2007 IEEE International Conference on Intelligent Robots and Systems, pp. 1801-1808, 2007.

[8] Issac Chang, "Finite Element Analysis of Hepatic Radiofrequency Ablation Probes using Temperature-Dependent Electrical Conductivity", Biomedical Engineering Online, 2:12, 2003.

[9] Anders Eriksson, "Influence of electrical and thermal properties on RF ablation of breast cancer: is the tumor preferentially heated?", Biomedical Engineering Online, 4:41, 2005.

[10] K. Archandran, "Electromagnetic and Thermal Simulation of 3-D Human Head Model under RF Radiation by Using the FDTD and FD Approaches", IEEE transactions on magnetics, Vol. 32, No. 3, pp. 1653-1656, 1996.

[11] Deshan Yang, "Measurement and Analysis of Tissue Temperature During Microwave Liver Ablation", IEEE transaction on biomedical engineering, Vol. 54, No. 1, pp. 150-155, 2007.

[12] Ping Liang et al, "Computer-Aided Dynamic Simulation of Microwave-Induced Thermal Distribution in Coagulation of the liver Cancer", IEEE transactions on biomedical engineering, Vol. 48, No. 7, pp. 821-828, 2001.

[13] Issac Chang, "Thermal modeling of lesion growth with radiofrequency ablation devices", Biomedical Engineering Online, 3:27, 2004.

[14] Fernando Bardati, "Time-Dependent Microwave Radiometry for the Measurement of Temperature in Medical Applications", IEEE transaction on microwave theory and techniques, Vol. 52, No. 8, 2004

[15] Masaki Fujimoto, "FDTD-Derived Correlation of Maximum Temperature Increase and Peak SAR in Child and Adult Head Models Due to Diapole Antenna", IEEE transactions on Electromagnetic, Vol. 48, No. 1, pp. 240-247, 2006.

[16] A. Hirata, M. Morita, T. Shiozawa, "Temperature Increase in the Human Head Due to a Dipole Antenna at Microwave Frequencies", IEEE transaction on Electromagnetic compatibility, Vol. 45, No. 1, pp. 109-116, 2003.

[17] Yilong Lu, Jianling Ying, Tat-Kee Tan, K. Arichandran, "Electromagnetic and Thermal Simulations of 3-D Human Head Model under RF Radiation by Using the FDTD and FD Approaches", IEEE transaction on Magnetics, Vol. 32, No. 3, pp. 1653-1656, 1996.

[18] H. H. .Pennes, "Analysis of Tissue and Arterial Blood Temperatures in the Resting Human Forearm", Journal of Applied Physiology, Vol. 1, No. 2, pp. 93-122, 1948.

[19] J. G. Webster, "Finite-Element Analysis of Hepatic Multiple Probe Radio-Frequency Ablation", IEEE Trans. Biomed. Eng., Vol. 49, No. 7, pp. 836-842, 2002.

[20] Patrick D. Wolf, "A Three-Dimensional Finite Element Model of Radiofrequency Ablation with Blood Flow and its Experimental Validation", Annals of Biomedical Engineering, Vol. 28, pp. 1075-1084, 2000.

[21] I. Tanasawa, K. Tanishita, "Genuine and Pseudo-ThermoPhysical Properties of Biological Media", International Journal of Thermophysics, Vol. 5, No. 2, pp. 149-160, 1984.

[22] J. W. Valvano, "Thermal Conductivity and Diffusion of Biomaterials Measured with Self-Heated Thermisters", International Journal of Thermophysics, Vol. 6, No. 3, pp. 301-311, 1985.

[23] Duck F, "Physical Properties of Tissue", A Comprehensive Reference Book, Academic Press, pp. 167-223, New York 1990.

[24] Tungjitkusolmun S., Staelin S. T., Haemmerich D., Tsai J. Z., Cao H., Webster J. G., Lee F. T., Mahvi D. M. and Vorperian V. R., "Three-dimensional finite-element analysis for radio-frequency hepatic tumor ablation", IEEE Trans Biomed Eng, Vol. 49, No. 1, pp. 3-9, 2002.